ELSEVIER

Journal of Alloys and Compounds 253–254 (1997) 162–166

Journal of ALLOYS AND COMPOUNDS

Hydrogen solubility limits in α- and β-zirconium

D. Khatamian*, V.C. Ling

AECL, Chalk River Laboratories, Stn. 82, Chalk River, ON, K0J-1J0 Canada

Abstract

Specimens of pure zirconium and Zr–20Nb alloy were charged to different hydrogen concentrations from the gas phase at 673 K. Before and after charging with hydrogen, the Zr–20Nb specimens were annealed in vacuum at 1123 K for 1 h and cooled to room temperature within about 30 min to produce a β-Zr structure. Some of these specimens were annealed further at 773 K for about 500 h to completely transform them to (α-Zr+β-Nb) phase. The specimens were analyzed for hydride transition temperatures using differential scanning calorimetry and for hydrogen concentration using hot vacuum extraction mass spectrometry. The hydrogen solubility limits found for pure Zr are in good agreement with the previously reported values. The solubility limits found in β-Zr are about two orders of magnitude higher than the solubility limits in α-Zr and the solubility limits found in the aged Zr–20Nb alloy are very close to those in α-Zr.

Keywords: Hydrogen; Solubility; α-Zirconium; β-Zirconium; CANDU

1. Introduction

In modern CANDU™ (CANada Deuterium Uranium) power reactors, pressure tubes of cold-worked Zr–2.5Nb (Zr–2.5 wt% Nb) material are used in the reactor core [1] to contain the fuel bundles and the heavy water (D_2O) coolant. The microstructure of the tubes consists of elongated α-Zr grains (~90%) surrounded by a network of β-Zr (~10%) with a composition of approximately Zr–20Nb (Zr–20 wt% Nb). The pressure tubes operate at temperatures ranging from ~520 K at the inlet to ~580 K at the outlet. Over time the pressure tubes absorb deuterium released by the corrosion reaction between the D_2O and the Zr. If the total hydrogen isotope concentration in the tubes exceeds the terminal solid solubility (TSS), the tubes can become susceptible to crack initiation and propagation by a process called delayed hydride cracking (DHC). Accurate values of the TSS are needed to ensure that DHC cannot occur in the pressure tubes during their operating lifetime. It has been shown that TSS in zirconium and its alloys displays a strong hysteresis and depends on whether hydrides are dissolving (TSSD) or precipitating (TSSP). The hydride dissolution temperature has a unique value, however, the hydride precipitation temperature depends, generally, on the maximum temperature to which the specimen is being heated and to a lesser degree on hold-time and cooling rate. Other variables that may affect TSS are the alloy composition and the microstructure [2–6]. In this paper, we report on measurements of the TSS in pure zirconium (α-Zr) and Zr–20Nb in its annealed (β-Zr) and fully aged (α-Zr+β-Nb) states [7,8]. These measurements were initiated to improve our understanding of TSS in the two phase pressure tube alloy Zr–2.5Nb.

2. Experimental

Specimens of pure zirconium (3×3×20 mm) and Zr–20Nb alloy (2×3×30 mm) were charged to different hydrogen concentration levels from the gas phase at 673 K. The pure Zr specimens were then homogenized at 673 K for 72 h. Prior to charging with hydrogen, the Zr–20Nb specimens were annealed in vacuum at 1123 K for 1 h and cooled to ambient temperature within about 30 min to convert the alloy to the β-Zr phase. The charging of these specimens was much faster than the α-Zr specimens, presumably due to the higher diffusion rate and the higher solubility limit for hydrogen in β-Zr [6]. After the charging process the Zr–20Nb specimens looked metallic and no surface hydride layer was apparent. The specimens were again annealed in separate quartz tubes, sealed under vacuum, at 1123 K for 1 h to make sure that they were homogenized with respect to hydrogen concentration and

*Corresponding author.

0925-8388/97/$17.00
PII S0925-8388(96)02947-7

that they completely transformed into β-phase [7]. Subsequent examination by X-ray diffraction confirmed that they had a β-Zr structure. Some of these specimens were aged in vacuum at 773 K for about 500 h [8]. After the aging, X-ray diffraction showed that they had completely transformed to (α-Zr+β-Nb) phase. Coupons of 3×3×2 mm size were cut from each specimen and used in the measurements.

The hydride dissolution temperatures on heatup of the specimens were measured using the Differential Scanning Calorimetry (DSC) technique. A TA Instruments DSC 2910[1] was used to perform the measurements. This instrument is based on a ''heat flux'' design which uses a constantan disk as primary means of transferring heat to the specimen and reference positions. As heat is transferred through the disk, the differential heat flow to the specimen and the reference is measured by area thermocouples formed by the junction of the constantan disk and chromel wafers which cover the underside of the specimen and reference platforms. Chromel and alumel wires attached to the chromel wafers form the thermocouples which directly measure the specimen temperature. In this case the reference was a hydrogen-free coupon of similar size, weight and the alloy composition to the specimen. The resulting differential heat flow reflected the dissolution/precipitation of hydrides in the specimen. Each specimen was analyzed for the phase transition temperature in at least three consecutive thermal cycle runs. The runs consisted of a heatup from ambient or a lower temperature to some maximum temperature, T_{max}, followed by a cooldown to the same lower temperature, with a hold-time of 5 min at T_{max}. The first run served to condition the specimens with the same thermal treatment immediately prior to any subsequent runs for which the results would be recorded. Since prior thermal history has an effect on the results, this procedure removed this uncertainty from the results. If the responses of the last two of three runs were similar, the results were deemed acceptable. For all the α-Zr and the aged Zr–20Nb specimens, T_{max} was chosen to be 723 K. However, in the case of the annealed Zr–20Nb (β-Zr) specimens the lowest possible T_{max} was used to minimize the potential transformation of meta-stable β-Zr structure. The highest T_{max} used was 523 K and, based on the Temperature Time Transformation (TTT) diagram [8], no transformation of the β-phase should have taken place during the DSC measurements. In all runs the heatup/cooldown rate was 30 K min^{-1}. The instrument was regularly calibrated using melting points of indium (429.76 K), tin (505.04 K) and lead (600.65 K). Following the DSC measurements, the specimens were analyzed for hydrogen concentration by the Hot Vacuum Extraction Mass Spectrometry (HVEMS) technique.

[1]TA Instruments Inc., 109 Lukens Drive, New Castle, DE 19720-0311, USA.

3. Results and discussion

3.1. α-Zr

The solubility limit for hydrogen in pure Zr was examined in the temperature range of 480–700 K. A typical heat flow curve with its temperature derivative is shown in Fig. 1. Three temperatures are marked in the figure; namely the Peak Temperature (PT), the Maximum Slope Temperature (MST) and the Completion Temperature (CT). In an ideally sharp transition these three temperatures are the same. However, in the case of metal/hydrogen systems, this is not true and, as the figure shows, they spread over ~30 K. Traditionally, due to ease of data analysis, MST, being about the average of the three temperatures, is taken as the hydride dissolution temperature [5]. Initially, in the present analysis as well, MST was taken as the hydride dissolution temperature (T_{TSSD}). The results of such analysis from pure zirconium specimens are plotted in Fig. 2(a). In the figure, the dashed line represents the best fit to the data and the solid line represents the results obtained by Kearns for unalloyed zirconium [3]. This figure shows that there is a large difference between the pure Zr data and Kearns' line. To explain this discrepancy one may argue that Kearns' line is the result of less accurate techniques used about three decades ago. On the other hand, it is possible that the discrepancy arises from the misinterpretation of the DSC heat flow signal or from errors in the hydrogen concentration measurements. In Fig. 2(b) the same data as in Fig. 2(a) are presented again. However, this time peak temperature (Fig. 1) has been assumed to be the hydride dissolution temperature, T_{TSSD}. In this case, as the Fig. 2(b) shows, the results are very close to the Kearns' line for unalloyed Zr and the discrepancy has disappeared. Motivated by these results, a set of coordinated DSC and neutron diffraction measurements were carried out to remove the uncertainty and identify the features of the heat flow signal that actually correspond to the hydride dissolution temperature. Neutron diffraction can remove this ambiguity because hydrides generate distinctive diffraction peaks whose intensity is directly proportional to the volume fraction of hydrides in the specimen. These measurements showed that for both α- and β-Zr the neutron diffraction results [9] for deuteride (the specimens were charged with deuterium instead of hydrogen in this specific cases) dissolution correlate, within the experimental errors, with the DSC peak temperature, PT. Therefore, PT was chosen as the TSSD temperature and used in the rest of the analyses.

The dashed line in Fig. 2(b) is determined by linear regression of log C_H versus $1/T$ (inverse temperature) and given by the following equation:

$$C_H = 1.46 \times 10^5 \exp(-3.73 \times 10^4/RT) \quad (1)$$

where C_H is in $\mu g\ g^{-1}$, T is in K and R, the universal gas

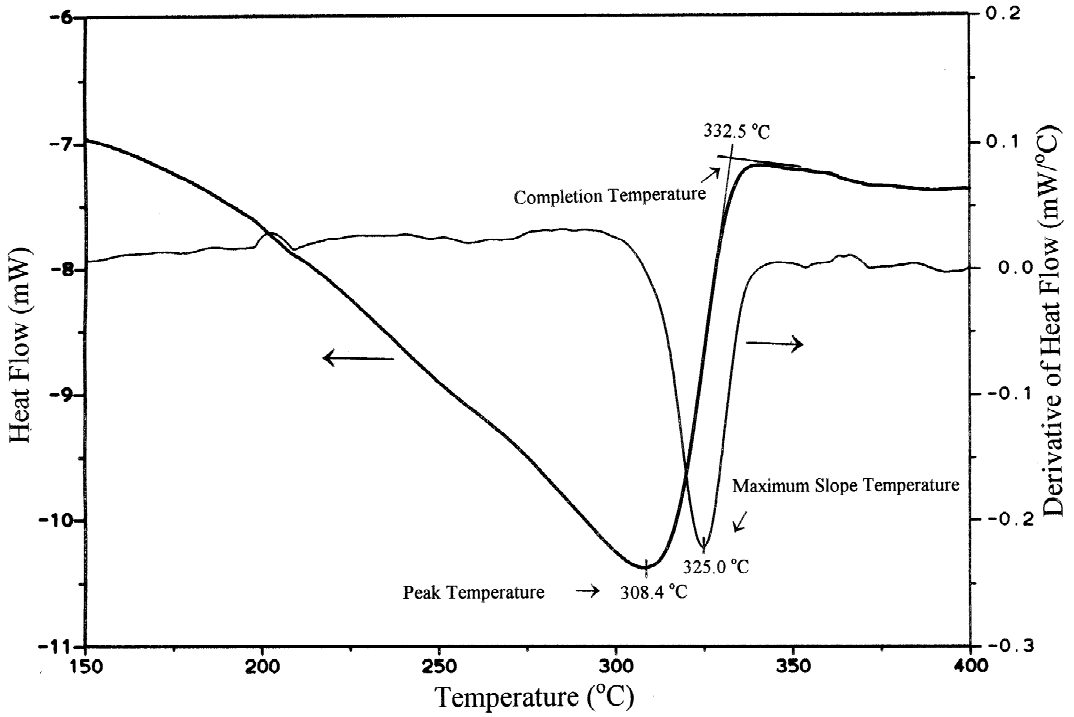

Fig. 1. DSC data from a α-Zr specimen containing 63±3 μg g^{-1} hydrogen obtained during heatup. Shown are the basic heat flow response and its temperature derivative.

constant, is 8.314 J K^{-1} mol^{-1}. The activation energy in Eq. (1) agrees very well with the value, 3.74×10^4 J mol^{-1}, obtained by Kearns [3].

3.2. Annealed Zr–20Nb (β-Zr)

The hydrogen solubility limits in β-Zr were examined in the temperature range of 220–470 K. The specimens with less than about 100 μg g^{-1} of hydrogen did not show any DSC signal for hydride dissolution. The reason for the absence of signal in these specimens is not known. The rest of the specimens, with higher hydrogen concentrations, displayed good DSC signals. The best fit to the data gives

$$C_H(\mu g\ g^{-1}) = 2.88\times10^4 \exp(-1.32\times10^4/RT) \qquad (2)$$

where R and T have the same meaning as in Eq. (1). The results are plotted in Fig. 3 along with the experimental

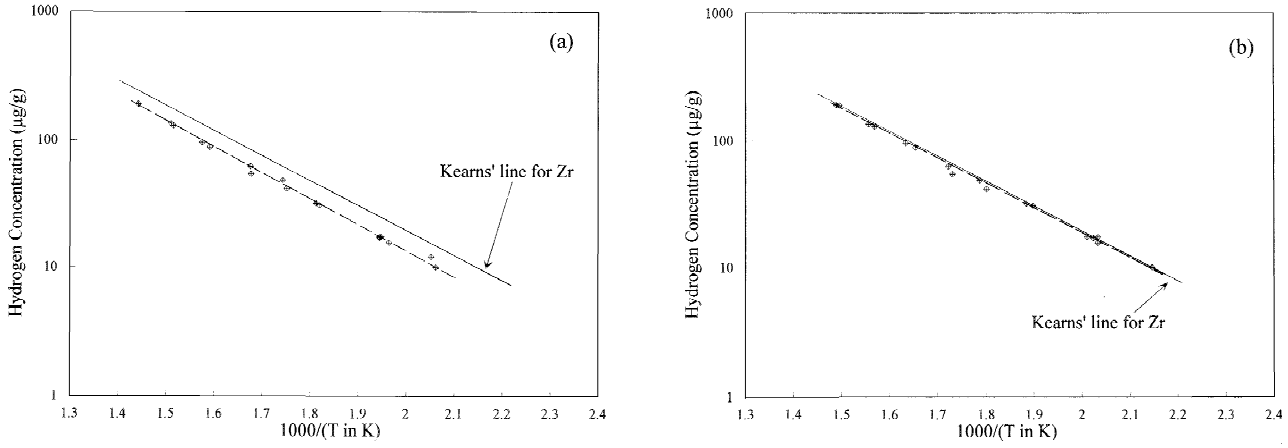

Fig. 2. TSSD for hydrogen in α-Zr. The results were obtained by assuming (a) MTS (see the text and Fig. 1) and (b) PT as the terminal hydride dissolution temperature. The dashed lines are the best fits to the data. Kearns' line for unalloyed Zr [3] is included for comparison.

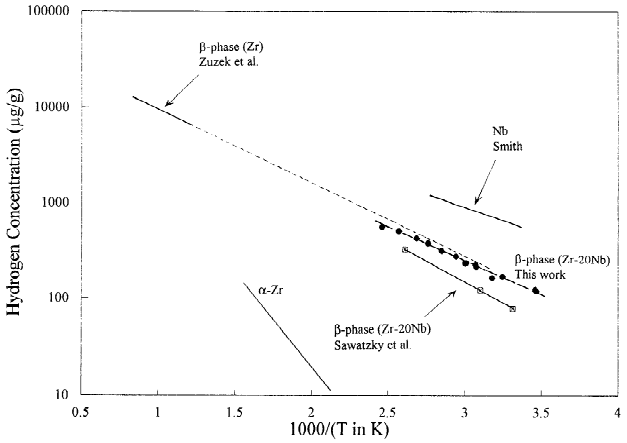

Fig. 3. TSSD for hydrogen in the annealed Zr–20Nb alloy (β-Zr) (solid circles). The experimental results of Sawatzky et al. for β-phase Zr–20Nb (open squares) [6], the hydrogen solubility limits for Nb [10] and high temperature β-Zr phase [2] are included for comparison.

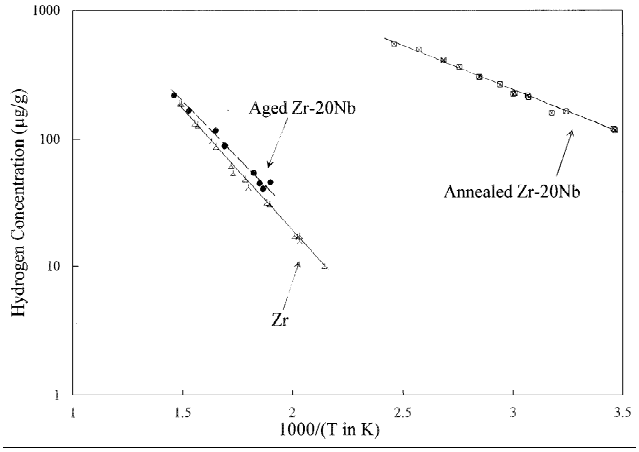

Fig. 4. TSSD for hydrogen in the aged Zr–20Nb alloy (solid circles). The hydrogen solubility limits in the annealed Zr–20Nb (open squares) and in pure Zr (open triangles) are included for comparison. The lines are the best fits to the data.

results of Sawatzky et al. for β-phase Zr-20Nb. Also the hydrogen solubility limits for Nb and high temperature β-Zr phase are included in the figure for comparison. These solubility limits are obtained from the H–Nb and H–Zr phase diagrams compiled by Smith [10] and Zuzek et al. [2] respectively.

Fig. 3 shows that the results of Sawatzky et al. are lower than the present measurements. The specimens of Sawatzky et al. were prepared by friction welding a hydrided piece to a similar unhydrided piece and annealing at a desired temperature for six weeks to achieve the equilibrium hydrogen distribution. The initially unhydrided piece was then analyzed for hydrogen to obtain TSSD at the annealing temperature. In such measurements, if the annealing period is not sufficient for the specimens to reach equilibrium, the final analysis will result in lower solubility limits. Also, at sufficiently high temperatures the meta-stable β-Zr phase may partially transform during annealing and result in lower solubility limits (see Section 3.3). The three data points reported indicate that the highest annealing temperature was ~383 K which according to the TTT diagram [8] is too low for any transformation to take place. Therefore, it seems to be more likely that the specimens did not reach equilibrium during annealing.

In Fig. 3 the extension of high temperature TSSD line for β-Zr (pure Zr with *bcc* structure) passes very close to the low temperature results reported here for β-phase Zr–20Nb (*bcc*). The figure also shows that, while the solubility limits in pure Nb (*bcc*) are only about four times higher than in β-Zr, the solubility limits in β-Zr are at least two orders of magnitude higher than those in α-Zr (*hcp*). This suggests that the TSS for hydrogen depends more on the crystal structure of this alloy than its composition.

3.3. Aged Zr–20Nb (α-Zr + β-Nb)

The hydrogen solubility limits in the aged Zr–20Nb alloy was examined in the temperature range of 500–700 K. The best fit to the data resulted in

$$C_{\mathrm{H}}(\mu\mathrm{g\ g}^{-1}) = 6.97 \times 10^{4} \exp(-3.26 \times 10^{4}/RT) \qquad (3)$$

Fig. 4 shows that the hydrogen solubility limits in the aged material is very close to the solubility limits in pure Zr, in spite of the fact that the alloy contains about 20% Nb. The solubility limit for hydrogen in Nb is about 3 orders of magnitude higher than in α-Zr, however, α-Zr has much higher affinity for hydrogen than Nb. To learn more about this problem and about the hydrogen solubility limits in Zr-Nb alloys, further measurements are underway using the β-annealed and the aged Zr-15Nb, Zr-10Nb, Zr-5Nb and Zr-2.5Nb alloys.

4. Conclusions

The solubility limits for hydrogen in pure zirconium (α-Zr), the β-annealed Zr–20Nb (β-Zr) and the aged Zr–20Nb (α-Zr + β-Nb) alloys have been measured using differential scanning calorimetry and hot vacuum extraction mass spectrometry. The solubility limits obtained for pure Zr are in good agreement with the results reported by Kearns [3] for unalloyed zirconium. The results also show that the solubility limits in β-Zr are about two orders of magnitude higher than the solubility limits in α-Zr and that the solubility limits in the aged Zr–20Nb alloy are very close to those in α-Zr.

Acknowledgments

Helpful discussions with V.F. Urbanic and A.A. Bahurmuz are acknowledged. The authors also wish to thank W.A. Ferris for charging the specimens with hydrogen. This work was funded by the Candu Owners Group (COG) under WPIR 3503.

References

[1] C.E. Ells, *Met. Soc. CIM* Annual Vol., 32 (1978).
[2] E. Zuzek, J.P. Abriata, A. San-Martin and F.D. Manchester, *Bull. Alloy Phase Diag., 11* (1990) 385.
[3] J.J. Kearns, *J. Nucl. Mater., 22* (1967) 292.
[4] G.F. Slattery, *J. Inst Metals, 95* (1967) 43 and *J. Nucl. Mater., 32* (1968) 30.
[5] D. Khatamian, Z.L. Pan, M.P. Pulls and C.D. Cann, *J. Aloys Comp., 231* (1995) 488.
[6] A. Sawatzky, G.A. Ledoux, R.L. Tough and C.D. Cann, *Proc. Mimami Int. Sym. Metal-Hydrogen Systems*, 13–15 April 1981, Miami Beach, Florida, T.N. Veziroglou (ed.), pp 109–120.
[7] J.P. Abriata and J.C. Bolcich, *Bull. Alloy Phase Diag., 3* (1982) 1711.
[8] B.A. Cheadle and S.A. Aldridge, *J Nucl. Mater., 47* (1973) 255.
[9] D. Khatamian and J.H. Root, details of these measurements will be published elsewhere.
[10] J.F. Smith, in T.B. Massalski, J.L. Murray, L.H. Bennett and H. Baker (eds.), *Binary Alloy Pliase Diagrams 2*, ASM, Metals Park, 1986, p. 1274.